www.ksmrm.org JKSMRM 17(1) : 41-46, 2013
Print ISSN 1226-9751

Case Report

Imaging Findings of Renal Cell Carcinoma Associated with Xp11.2 Translocation/TFE3 Gene Fusion in a 4-Year-Old Male: Case Report and Review of Literature

Hyun Gi Kim[1], Mi-Jung Lee[1], Sarah Lee[2], Myung-Joon Kim[1], Chang Hee Hong[3]

[1]Department of Radiology and Research Institute of Radiological Science, Severance Children's Hospital, Yonsei University, College of Medicine

[2]Department of Pathology, Severance Hospital, Yonsei University, College of Medicine

[3]Department of Pediatric Urology, Severance Children's Hospital, Yonsei University, College of Medicine

We represent a pathologically proven case of a four-year-old male patient with renal cell carcinoma associated with Xp11.2 translocation/TFE3 gene fusion, which is rare but more frequent in children or young adults. Computed tomography showed about 2.5 cm size ill-defined mass in the right kidney. The mass was hyperechoic on ultrasound. Magnetic resonance imaging demonstrated a mass with capsular enhancement and diffusion restriction. We present a case of Xp11.2 renal cell carcinoma and provide review of the literature.

Index words : Renal cell carcinoma · Xp11.2 translocation · TFE3 gene fusion · Diffusion-weighted MRI · Child

INTRODUCTION

While Wilms' tumor accounts for 87% of all pediatric renal masses, pediatric renal cell carcinoma (RCC) is rare. RCC in children or young adults is often hereditary and is associated with von Hippel-Lindau syndrome. Sporadic RCC in children or young adults is less common and is often associated with Xp11.2 translocation/TFE3 gene fusion. The proportion of Xp11.2 translocation/TFE3 gene fusion RCC (Xp11.2 RCC) among RCC in young age group varies from 20% to 70%. Although several studies about pathologic features of Xp11.2 RCC have been reported (1), its radiological imaging findings are not yet fully understood. We report a case of a pediatric Xp11.2 RCC, emphasizing the radiological aspects, including ultrasound (US), computed tomography (CT), and magnetic resonance (MR) imaging with diffusion-weighted imaging (DWI) and dynamic enhancement.

• Received; February 14, 2012 • Revised; May 15, 2012
• Accepted; July 5, 2012

Corresponding author : Myung-Joon Kim, M.D., Department of Radiology and Research Institute of Radiological Science, Severance Children's Hospital, Yonsei University, College of Medicine, 250 Seongsanno (134 Sinchon-dong), Seodaemun-gu, Seoul 120-752, Korea. Tel. 82-2-2228-7400, Fax. 82-2-393-3035, E-mail : mjkim@yuhs.ac

CASE REPORT

A four-year-old boy with no specific birth or other past history presented with intermittent gross hematuria that had persisted for one year. Urine analysis showed proteinuria, hematuria, and dysmorphic red blood cells.

Single excretory phase CT (Brilliance 64; Philips Medical Systems, Cleveland, OH, USA) with contrast enhancement was performed at an outside hospital. The CT scan showed an ill-defined mass of 24 × 19 × 16 mm size in the lower pole of the right kidney involving renal pelvis (Fig. 1a). The lesion showed lower attenuation than the surrounding renal parenchyma with heterogeneous enhancement. Although pre-contrast images were not obtained, there

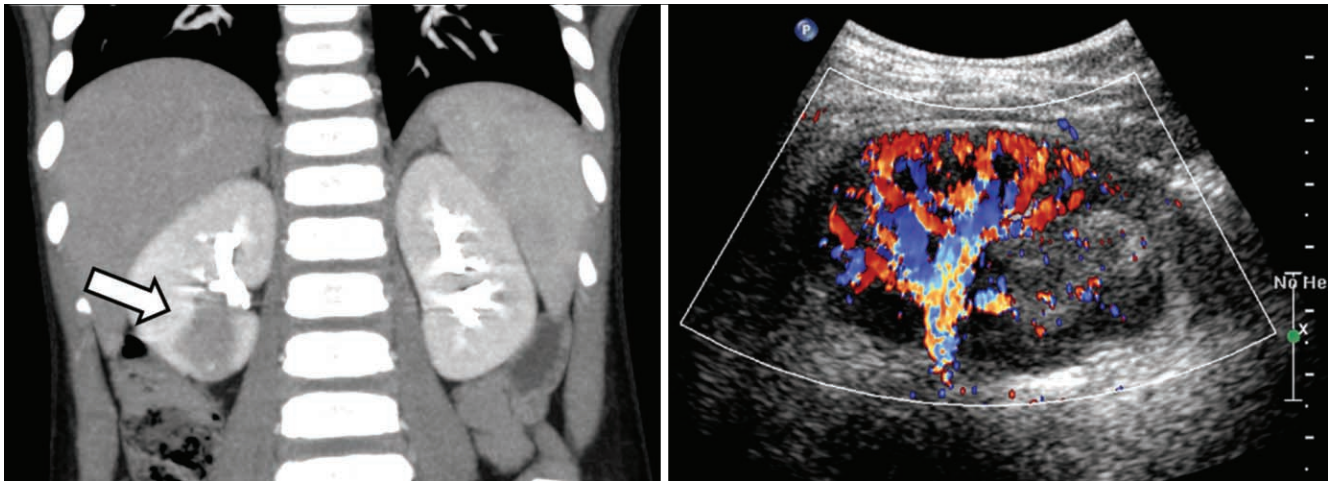

a b

Fig. 1. Coronal image of an enhanced computed tomography scan shows an ill-defined hypodense tumor of the right kidney involving the renal pelvis (a). Under Doppler imaging, hyperechoic mass invading the renal cortex and sinus shows hypovascularity compared with the surrounding normal parenchyma (b).

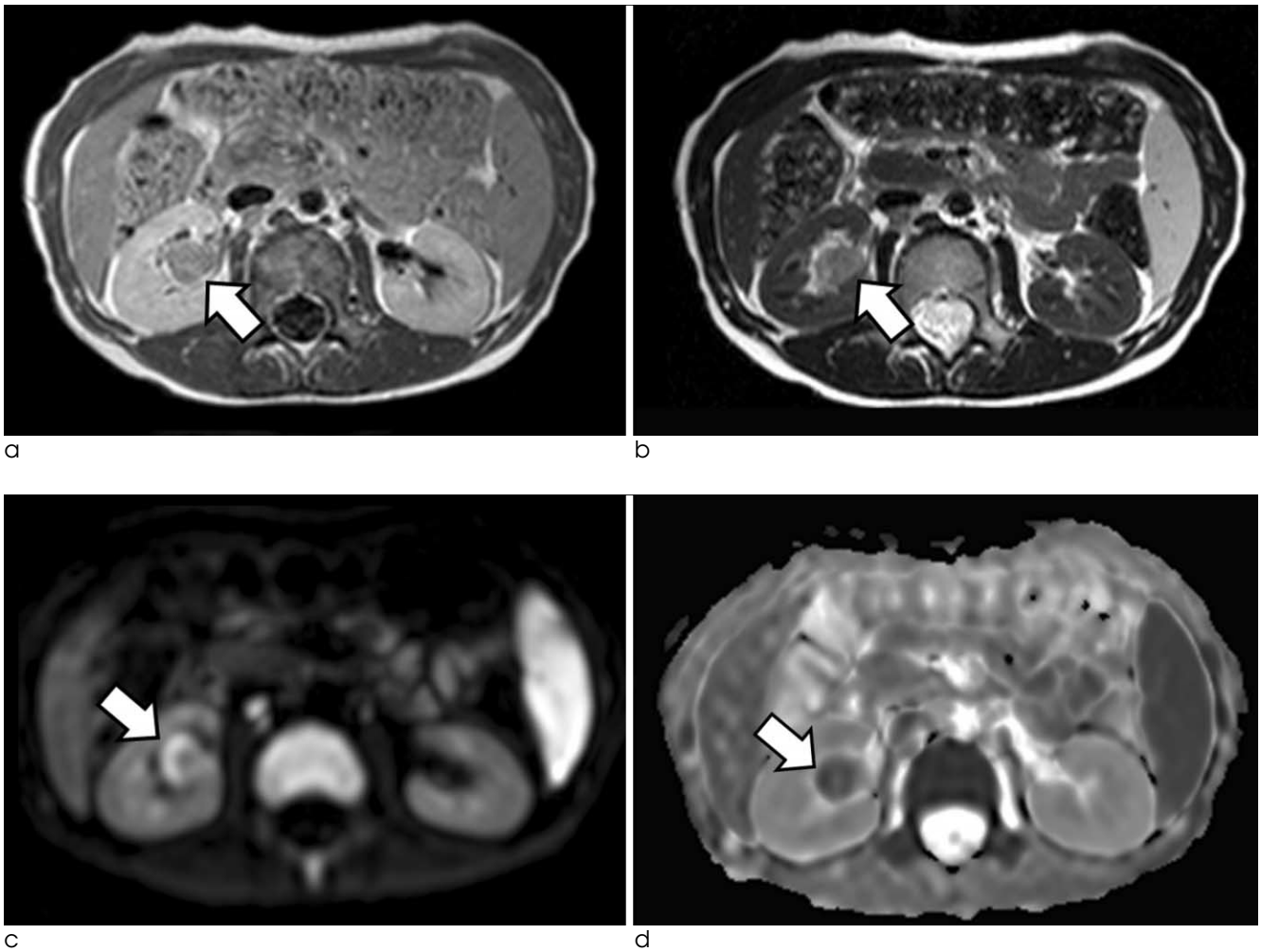

a b

c d

Fig. 2. On magnetic resonance images, the renal mass shows low to intermediate signal intensity on T1-weighted imaging (a) and intermediate to high signal intensity on T2-weighted imaging (b). On diffusion-weighted imaging, peripheral high signal intensity is shown (b = 1000 sec/mm^2) (c). The same peripheral area was of low signal intensity on the apparent diffusion coefficient map (d).

was no definite calcification in the mass.

After the patient was transferred to our hospital, US and MR imaging were performed for further evaluation. US evaluation (iU-22; Philips Medical Systems, Best, The Netherlands) revealed lobulated and hyperechoic mass invading the renal cortex and the renal sinus (Fig. 1b). When Doppler imaging was applied, the mass was found to be hypovascular compared to the surrounding normal parenchyma.

MR imaging was performed using a 1.5T scanner (Intera Achieva; Philips Medical System, Best, The Netherlands) equipped with a SENSE cardiac coil. Conventional imaging with DWI was performed and Gd-DOTA (Dotarem, Guerbet, Aulnay-sous-Bois, France) was used for the dynamic contrast enhancement study. The tumor was of low to intermediate signal intensity on T1-weighted images (Fig. 2a) and of intermediate to high signal intensity on T2-weighted images (Fig. 2b). DWI was obtained using b values of 0, 500, and 1000 sec/mm^2, and the peripheral portion of the mass showed diffusion restriction compared to the central part of the mass (Fig. 2c). The mean value of the apparent diffusion coefficient (ADC) in the tumor with diffusion restriction was lower than the surrounding normal renal parenchyma (1.043×10^{-3} and 2.061×10^{-3} mm^2/sec, respectively) (Fig. 2d). As part of the dynamic phase, corticomedullary, nephrographic, and delayed phases were obtained at 20, 40, and 60 seconds after contrast injection, respectively. During the dynamic enhancement study, the renal mass showed less enhancement than the normal renal parenchyma (Fig. 3a–d) and showed peripheral enhancement on corticomedullary phase (Fig. 3b). There was no evidence of regional lymph node or

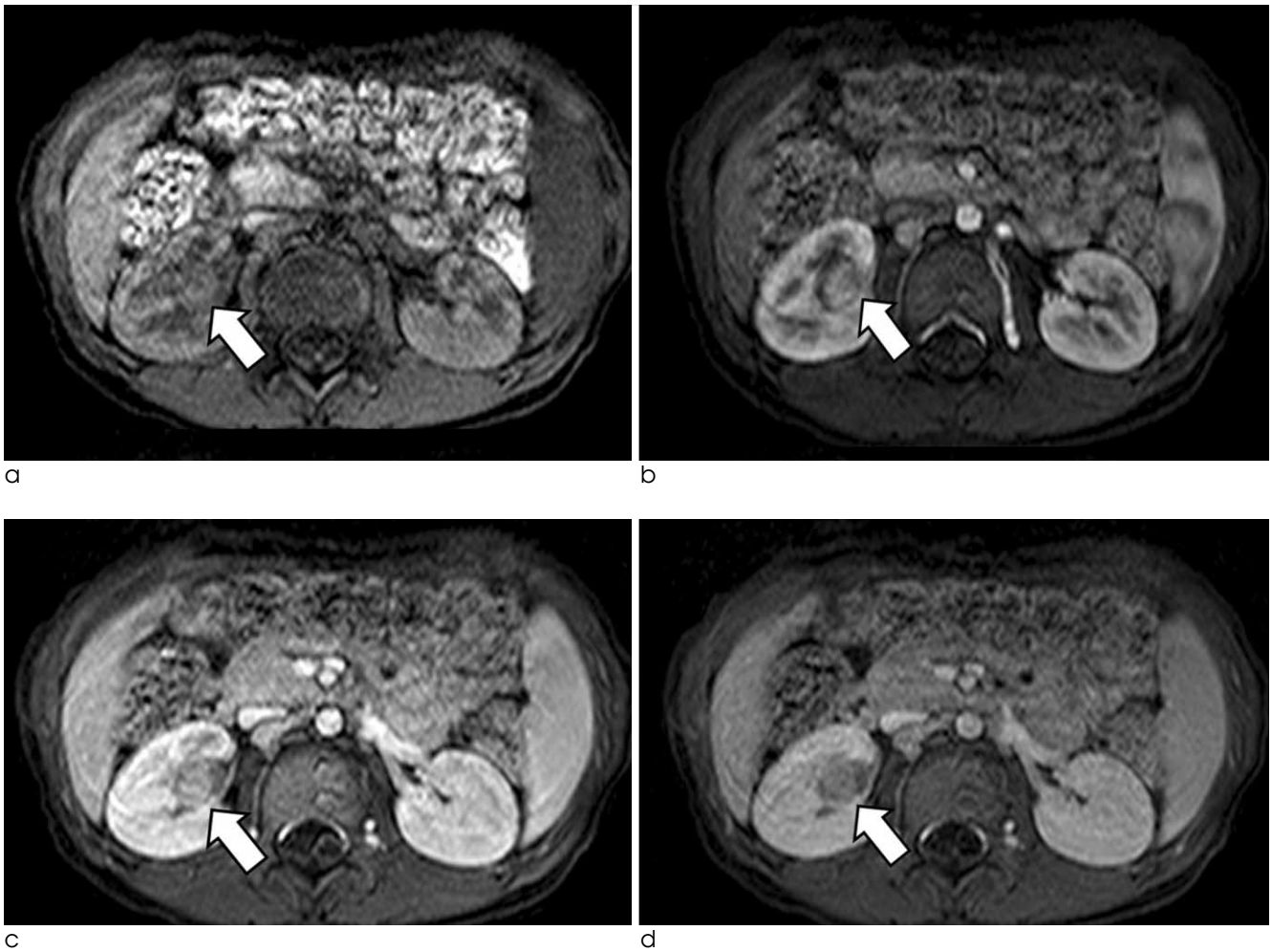

Fig. 3. Dynamic enhancement study on T1-weighted images including precontrast (a), corticomedullary (b), nephrographic (c), and delayed phases (d). The mass shows lower signal intensity than the normal renal parenchyma on all phases; however, it shows heterogeneous enhancement.

distant metastasis on pre-operative radiologic evaluations.

Along with Wilms' tumor, which is the most common renal mass in pediatric patients, other tumors such as inflammatory myofibroblastic tumor of renal pelvis, leiomyoma, solitary fibrous tumor, and RCC was included in the differential diagnosis. As the mass was not showing typical features of Wilms' tumor and the possibility of malignancy had to be ruled out before total nephrectomy, US-guided percutaneous biopsy was performed before the open surgery. After frozen specimen was confirmed as a malignant tumor, right nephrectomy was performed. Renal capsule was intact and there was no adhesion between the kidney and the surrounding structures.

Gross specimen showed infiltrative yellow mass (24 × 10 mm) in the lower pole of the right kidney which contained necrotic lesion in central and renal pelvic area. The mass was 4 mm apart from the capsule and was abutting on the calyx. Parenchymal congestion was noted at the inferior side of the mass and there was partial capsule formation (Fig. 4a). On microscopic evaluation, the tumor was predominantly of clear cell type with papillary figures and psammomatous calcifications (Fig. 4b). Calcifications were dominant in the peripheral portion of the tumor. Immunohistochemical staining showed that the nuclei of tumor cells were immunoreactive for TFE3 (Fig. 4c). The final pathologic diagnosis was Xp11.2 RCC.

Overall TNM staging was stage 1 as T1N0M0. Follow up imaging of positron emission tomography and US showed no evidence of tumor recurrence or metastasis until 21 months after the surgery.

DISCUSSION

Wilms' tumor is the most common renal tumor in

a

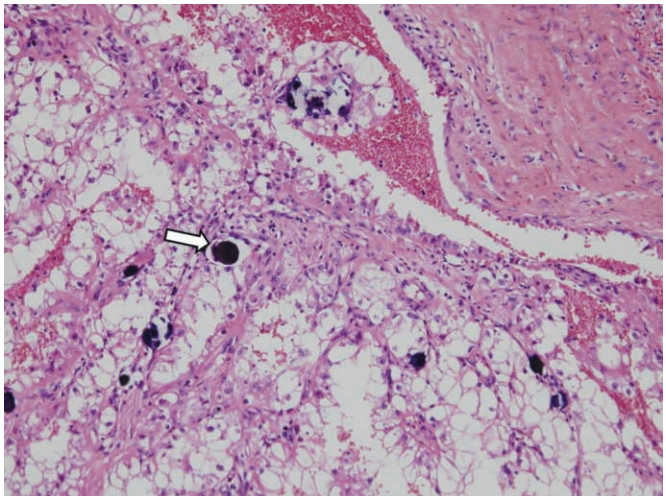

b

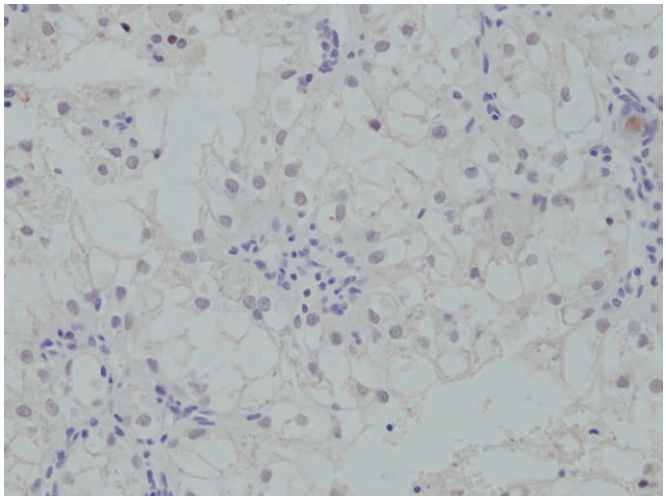

c

Fig. 4. Gross specimen shows infiltrative mass containing necrotic lesion in the lower pole of the right kidney (**a**). Histopathological photomicrograph shows papillary pattern with voluminous clear cells and psammomatous calcification (arrow) (Hematoxylin & Eosin stain, original magnification, × 100) (**b**). Immunohistochemical staining shows strong nuclear expression of TFE3 (original magnification, × 200) (**c**).

children, but mesoblastic nephroma, rhabdoid tumor, and clear cell sarcoma can also occur in young age group. Because RCC occurs infrequently in children, it is generally hard to differentiate RCC from Wilms' tumor before histopathologic confirmation. While the peak patient age at presentation of Wilms' tumor is three years, the mean age of the presentation of RCC is approximately eight to nine years (3). Compared with Wilms' tumor, RCC manifests more bilaterally (2). If RCC tends to be multiple, von Hippel-Lindau syndrome should be ruled out in pediatric patients (4). Generally, clear cell RCC is the most common histologic subtype, accounting for 70% of all RCC. However, pediatric population tends to have more proportion of papillary carcinoma than clear cell RCC (5).

Xp11.2 RCC was described as an independent entity in the 2004 World Health Organization classification of kidney tumors. This carcinoma predominantly affects young age group from children to the second and third decades of life generally showing no gender predominance. It has a wide morphologic spectrum on histopathology with both clear cells and papillary architecture and often with abundant psammoma bodies (6). Xp11.2 RCC is reported to consist 20 – 70% of RCC in young patients (5, 7). Grossly, Xp11.2 RCC is indistinguishable from conventional RCC and the radiological findings of Xp11.2 RCC are unspecific.

RCC is characterized by rich blood flow and vascularity. Color Doppler images of our case showed minimal blood flow in comparison with the adjacent renal parenchyma. On contrast enhanced study of CT, however, it showed heterogeneous enhancement. No particular enhancement pattern of Xp11.2 RCC is reported yet, however, thick peripheral rim enhancement was noted in the previous report, which was similar to our case (9). There was mild and delayed enhancement in the periphery of the lesion in our case and this is believed to be caused by partial capsule formation . In another case report of Xp11.2 RCC of an adult patient, the tumor was hyperdense but did not show distinct enhancement on CT (8).

MR imaging can be used to characterize and differentiate renal masses including RCC. The MR findings of RCC are similar to those of Wilms' tumor. Generally, RCC can appear as iso- or hypointense on T1-weighted images and has variable signal intensities on T2-weighted images. There are few reports dealing with MR imaging findings of Xp11.2 RCC in young age group. A previous Xp11.2 RCC case showed partially solid and cystic portion in the mass on MR imaging (10). Our case showed intermediate to high signal intensity on T2-weighted images, but there was no definite cystic component. Central part of the mass showing less diffusion restriction could be explained by central necrosis confirmed from gross specimen.

DWI can be helpful for differentiating subtypes of RCC. However, there have been few studies about the use of DWI in Xp11.2 RCC. Our study showed a low ADC value in the tumor, especially in the peripheral portion (1.043×10^{-3} mm^2/sec). However, DWI of Xp11.2 RCC in a previous report was isointense compared with renal parenchyma (9). Further study is needed to refine this aspect.

Grossly, Xp11.2 RCC can have either well-demarcated or irregular margin (9–11). Our case showed irregular and infiltrative margin both in the imaging studies and in the gross specimen. However, the mass was located inside the kidney contour and did not extend across the perinephric area.

Like acute leukemia, Xp11.2 RCC is associated with exposure to prior chemotherapy (12). However, there was no history of prior chemotherapy in our patient. Prognosis of Xp11.2 RCC in children or young adults is still controversial. However, recent studies have shown that Xp11.2 RCC is associated with significantly decreased disease-free and overall survival (13, 14). Our case was followed-up until 21 months after surgery and showed no evidence of tumor recurrence or metastasis.

This report is a case of rare renal malignancy occurred in a four-year-old boy. As Xp11.2 RCC has a variety of histopathologic findings, typical radiologic features have not yet been characterized. This is the first case report showing all of the US, CT, and MR imaging characteristics, including DWI and dynamic enhancement. Although RCC is rare in children, if renal mass does not show typical findings of Wilms' tumor, Xp11.2 RCC should be considered as one possible differential diagnosis. Further evaluation and reports should be needed to acquire characteristic radiological findings of this tumor.

References

1. Ross H, Argani P. Xp11 translocation renal cell carcinoma. Pathology 2010;42:369-373
2. Geller E, Smergel EM, Lowry PA. Renal neoplasms of childhood. Radiol Clin North Am 1997;35:1391-1413
3. Dehner LP, Leestma JE, Price EB, Jr. Renal cell carcinoma in children: a clinicopathologic study of 15 cases and review of the literature. J Pediatr 1970;76:358-368
4. Hartman DS, Davis CJ, Jr., Madewell JE, Friedman AC. Primary malignant renal tumors in the second decade of life: wilms tumor versus renal cell carcinoma. J Urol 1982;127:888-891
5. Bruder E, Passera O, Harms D, et al. Morphologic and molecular characterization of renal cell carcinoma in children and young adults. Am J Surg Pathol 2004;28:1117-1132
6. Argani P, Olgac S, Tickoo SK, et al. Xp11 translocation renal cell carcinoma in adults: expanded clinical, pathologic, and genetic spectrum. Am J Surg Pathol 2007;31:1149-1160
7. Dal Cin P, Stas M, Sciot R, De Wever I, Van Damme B, Van den Berghe H. Translocation (X; 1) reveals metastasis 31 years after renal cell carcinoma. Cancer Genet Cytogenet 1998;101: 58-61
8. Yamaguchi T, Kuroda N, Imamura Y, Hes O, Kawada T, Nakayama K. Imprint cytologic features in renal cell carcinoma associated with Xp11.2 translocation/TFE3 gene fusion in an adult: a case report. Acta Cytol 2009;53:693-697
9. Kato H, Kanematsu M, Yokoi S, et al. Renal cell carcinoma associated with Xp11.2 translocation/TFE3 gene fusion: radiological findings mimicking papillary subtype. J Magn Reson Imaging 2011;33:217-220
10. Jayasinghe C, Siegler N, Leuschner I, Fleischhack G, Born M, Muller AM. Renal cell carcinoma with Xp11.2 translocation in a 7-year-old boy. Klin Padiatr 2010;222:187-189
11. Winarti NW, Argani P, De Marzo AM, Hicks J, Mulyadi K. Pediatric renal cell carcinoma associated with Xp11.2 translocation/TFE3 gene fusion. Int J Surg Pathol 2008;16:66-72
12. Argani P, Lae M, Ballard ET, et al. Translocation carcinomas of the kidney after chemotherapy in childhood. J Clin Oncol 2006;24:1529-1534
13. Wu A, Kunju LP, Cheng L, Shah RB. Renal cell carcinoma in children and young adults: analysis of clinicopathological, immunohistochemical and molecular characteristics with an emphasis on the spectrum of Xp11.2 translocation-associated and unusual clear cell subtypes. Histopathology 2008;53:533-544
14. Qiu R, Bing G, Zhou XJ. Xp11.2 Translocation renal cell carcinomas have a poorer prognosis than non-Xp11.2 translocation carcinomas in children and young adults: a meta-analysis. Int J Surg Pathol 2010;18:458-464

대한자기공명의과학회지 17:41-46(2013)

4세 남아에서 발견된 Xp11.2 염색체 재배열/TFE3 유전자 융합 연관 신세포암의 영상 소견: 증례보고 및 문헌고찰

[1]연세대학교 의과대학 세브란스병원 영상의학과
[2]연세대학교 의과대학 세브란스병원 병리학과
[3]연세대학교 의과대학 세브란스병원 소아비뇨기과

김현지[1] · 이미정[1] · 이사라[2] · 김명준[1] · 홍창희[3]

신세포암의 여러 종류 중 Xp11.2 염색체 재배열/TFE3 유전자 융합 연관 신세포암은 드물며 소아나 젊은 성인에서 더 흔한 것으로 알려져 있다. 이 증례보고는 병리학적으로 확인된 4세 남자 환자의 Xp11.2 염색체 재배열/TFE3 유전자 융합 연관 신세포암에 대한 것이다. 본 증례에서 종양은 컴퓨터 단층 촬영에서 우측 신장에 2.5 cm 크기의 경계가 불명확한 종괴로 보였으며, 초음파상 고에코 병변으로 보였다. 자기공명영상에서는 종괴 캡슐의 조영증강과 함께 종괴의 확산 제한이 보였다. 저자들은 이 드문 신세포암의 영상 소견에 대해 증례를 보고하고 문헌을 고찰하는 바이다.

통신저자 : 김명준, (120-752) 서울시 서대문구 연세로 50 (신촌동134), 연세대학교 의과대학 세브란스병원 영상의학과
Tel. (02) 2228-7400 Fax. (02) 393-3035 E-mail: mjkim@yuhs.ac